JCTC Journal of Chemical Theory and Computation

DFT Method Estimation of Standard Redox Potential of Metal Ions and Metal Complexes[†]

Yoshiki Shimodaira,[‡] Toshiko Miura,[§] Akihiko Kudo,[‡] and Hisayoshi Kobayashi*,[§]

Department of Applied Chemistry, Faculty of Science, Science University of Tokyo, 1-3 Kagurazaka, Shinjuku-ku, Tokyo 162-8601, Japan, and Department of Chemistry and Materials Technology, Kyoto Institute of Technology, Matsugasaki, Kyoto 606-8585, Japan

Received January 13, 2007

Abstract: The DFT method calculation was carried out to evaluate standard redox potential (SRP) for metal-to-metal cation and metal-to-metal complex systems. With the Born–Haber cycle, standard redox potential was composed of the cohesive energy, ionization energy, and solvation energy. The ligand exchange energy was added in case of metal complex. The solvent effects were incorporated by the self-consistent reaction field theory at the level of the polarized continuum model (PCM). At the highest level of calculations, the geometry optimization and harmonic frequency analysis were evaluated under the PCM. Utilizing experimental values of the cohesive energy of metals, the standard deviations between the calculated and experimental SRP values were 0.20–0.27 V depending on the calculation levels and basis sets used. For three Ag complexes with CN^-, $S_2O_3^{2-}$, and NH_3 ligands, the discrepancy was within 0.3 V.

Introduction

Although the standard redox potential (SRP) determining the equilibrium between bulk metal and metal ion or metal complex is the most fundamental quantity in electrochemistry, computational chemistry approach has not been carried out so far. The SRP corresponds to a process in which a metal ion begins to be deposited on the solid metal electrode soaking in acid solution and to be reduced. However, it is easily anticipated that many factors relating adsorption and coordination of solvent molecules to metal surfaces and to metal ions influence the process in a complicated manner. In recent years, quantum chemical methodology for the solution chemistry has developed.[1-3] Techniques managing solvent as continuum models have been established and incorporated in many molecular orbital (MO) and density functional theory (DFT) method programs. It means that new approaches on electrochemistry become possible. A straightforward application is evaluation of solvation free energy,

and many papers have been published so far.[4-8] Baik and Friesner estimated the redox potentials for organic molecules and metal complexes.[9] Undsemaa and Tamm calculated the redox potentials for oxidation number change of transition-metal ions.[10] They also presented the structure of hydration spheres.

In this study, we try to evaluate the SRP for 21 metal ions (metal aqueous complexes) such as Li^+, K^+, Ca^{2+}, Na^+, Mg^{2+}, Al^{3+}, Ti^{2+}, Mn^{2+}, Zn^{2+}, Cr^{3+}, Fe^{2+}, Co^{2+}, Ni^{2+}, Fe^{3+}, Cu^{2+}, Cu^+, Ag^+, Pd^{2+}, Pt^{2+}, Au^{3+}, and Au^+ in the increasing order of experimental SRP values[11] and three Ag complexes with nonaqueous ligands, $[Ag(NH_3)_2]^+$, $[Ag(CN)_2]^-$, and $[Ag(S_2O_3)_2]^{3-}$, based on the DFT calculations. The redox potentials for the oxidation number change of a transition-metal complex, such as $[Fe(CN)]^{3-} + e^- \rightarrow [Fe(CN)]^{4-}$, have been reported by other researches.[9,10] Those calculations require only the isolated complexes. However, for silver complexes, the oxidation number becomes zero when reduced. So some device is necessary, and our approach is applicable for this case.
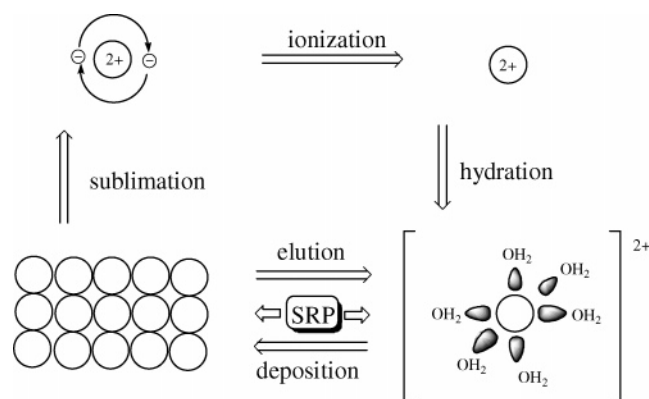
To get an image of change of states easily, we consider the opposite direction of the process, i.e., the process from solid metal to hydrated metal ion. This process is partitioned into the three processes utilizing the Born–Haber cycle

---

[†] Dedicated to Professor Dennis R. Salahub on the occasion of his 60th birthday.

* Corresponding author e-mail: kobayashi@chem.kit.ac.jp.

[‡] Science University of Tokyo.

[§] Kyoto Institute of Technology.

Scheme 1. Born−Haber Cycle and SRP Process

(6+0) (4+2) (2+4)

Figure 1. Schematic illustration of three aqueous metal complexes. Six coordination octahedral structure, four coordination tetrahedral structure with two water molecules in the second coordination shell, and two coordination linear structure with four water molecules in the second coordination shell. Their coordination modes are abbreviated as (6 + 0), (4 + 2), and (2 + 4), respectively.

(Scheme 1): (1) sublimation or cohesion to atoms from solid, (2) ionization of atoms, and (3) formation of a hydrated complex from the bare ion and water molecules. For the case of the metal-to-metal complex, (4) the ligand exchange process is added. The SRPs are estimated as the sum of energy changes for the three or four processes. The usefulness of our approach has been demonstrated in a preliminary report.[12]

Method of Calculation and Models
Equation 1 shows the energy change from bulk metal to hydrated metal ion shown in Scheme 1.

$$\Delta\epsilon = \epsilon_{\text{cohe}}^{\text{expt}} + \epsilon_{\text{ion}} + \epsilon_{\text{hydra}}(+ \epsilon_{\text{li−ex}}) \tag{1}$$

The first term on the right-hand side $\epsilon_{\text{cohe}}^{\text{expt}}$ is the sublimation process from solid to gas. This quantity is equivalent to the cohesive energy, which could be evaluated as an energy difference between a bulk solid and an isolated atom if band calculation is carried out. Since the other processes are able to be evaluated within a molecular model, and the purpose of the present work is not to evaluate the cohesive energy precisely, experimental values of the cohesive energy are employed.[13] The second term ϵ_{ion} and the third term ϵ_{hydra} on the right-hand side are ionization energy and hydration energy, respectively. The present method is also applied to Ag complexes with nonaqueous ligands. Then the forth term $\epsilon_{\text{li−ex}}$ representing the ligand exchange energy is added.

There are two approaches to estimate the ionization energy. One is to calculate the energy difference between a neutral atom and its cation (so-called ΔSCF method), as shown in eq 2a, using the same functional and basis set as the rest of the calculation (e.g., hydration energy). In another approach, experimental values of the ionization energy are employed as shown in eq 2b. These are referred to as theoretical and experimental estimation of ionization energies.

$$\epsilon_{\text{ion}} = \epsilon[M^{n+}] - \epsilon[M^0] \tag{2a}$$

$$\epsilon_{\text{ion}} = \epsilon_{\text{ion}}^{\text{expt}} \tag{2b}$$

$$\epsilon_{\text{hydra}} = \epsilon[M(OH_2)_6{}^{n+}] - \epsilon[M^{n+}] - \epsilon[6H_2O] \tag{3}$$
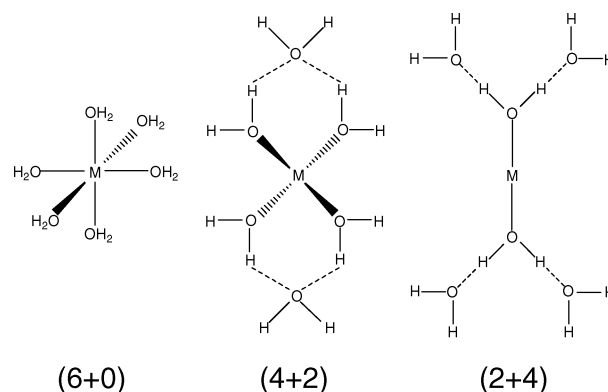
The hydration energy is expressed in eq 3. In this calculation, six water molecules are arranged around the metal cation, and the hydration energy is the difference between the energy of an aqueous metal complex and the sum of energies of a bare cation and an aqueous cluster composed of six water molecules. Three types of coordination modes of aqueous complexes are considered as shown in Figure 1: (1) six coordination octahedral structure, (2) four coordination tetrahedral structure with two water molecules in the second coordination shell, and (3) two coordination linear structure with four water molecules in the second coordination shell. Their coordination modes are abbreviated as (6 + 0), (4 + 2), and (2 + 4), respectively. The two or four water molecules in the second coordination shell have no realistic evidence. However the use of (4 + 2) and (2 + 4) modes rather than (4 + 0) and (2 + 0) modes can restrict the reference system to 6H$_2$O only. For individual metals, the most stable configuration is determined by optimizing the three coordination modes of an aqueous complex in gas-phase and then by recalculating their total energies in solution.
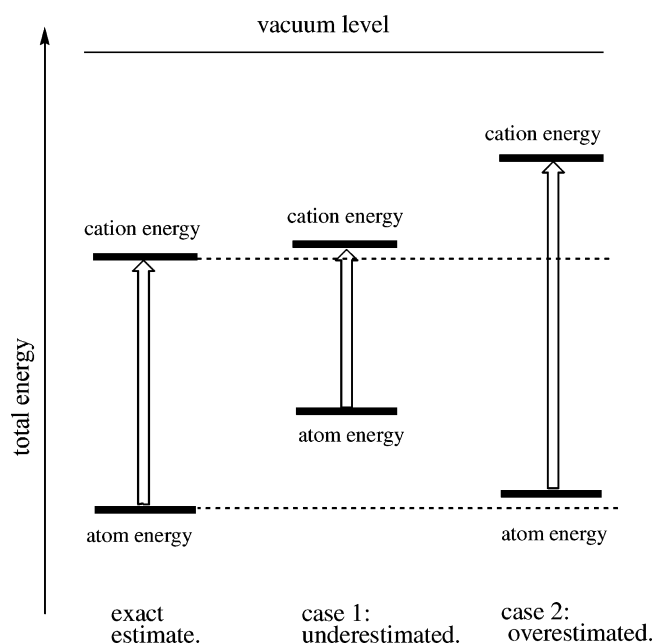
$$\Delta\epsilon = \epsilon_{\text{cohe}}^{\text{expt}} + \epsilon_{\text{ion}} + \epsilon_{\text{hydra}}$$

$$= \epsilon_{\text{cohe}}^{\text{expt}} + (\epsilon[M^{n+}] - \epsilon[M^0]) + (\epsilon[M(OH_2)_6{}^{n+}] - \epsilon[M^{n+}] - \epsilon[6H_2O]) \tag{4a}$$

$$= \epsilon_{\text{cohe}}^{\text{expt}} - \epsilon[M^0] + \epsilon[M(OH_2)_6{}^{n+}] - \epsilon[6H_2O]$$

$$\Delta\epsilon = \epsilon_{\text{cohe}}^{\text{expt}} + \epsilon_{\text{ion}}^{\text{expt}} + \epsilon[M(OH_2)_6{}^{n+}] - \epsilon[M^{n+}] - \epsilon[6H_2O] \tag{4b}$$

The total energy change is expressed in eqs 4a or 4b, depending on the estimation of the ionization energy. In the theoretical estimation scheme (eq 4a), the energy of the metal ion appears twice in the opposite sign, and these terms are canceled. Only the energy of the metal atom is left in the final equation. On the other hand, only the energy of the

DFT Method Estimation of Standard Redox Potential

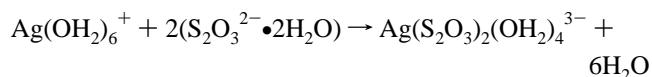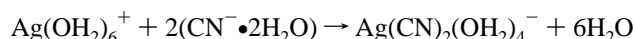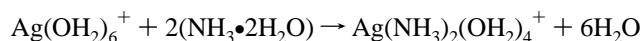*J. Chem. Theory Comput., Vol. 3, No. 3, 2007* **791**

Scheme 2. Origin of Errors in Ionization Energy Calculation

metal cation appears in eq 4b. We adopt both the estimation schemes mixed. This reasoning is discussed below.

One origin of numerical errors comes from the inaccuracy in the total energies of metal atom and cation. This situation is illustrated in Scheme 2. Because of the variational principle, the energy levels for atoms and cations are never calculated deeper than their exact energy levels. It means that the errors are classified into two cases. In case 1, underestimation of the ionization energy suggests that the energy of atom is evaluated more poorly (higher in energy). In case 2, overestimation of the ionization energy suggests that the energy of cation is evaluated too much upward. The cation energy and atom energy are relatively more reliable in case 1 and case 2, respectively, and therefore the adoption of the experimental estimation scheme for case 1 (since it depends on the cation energy only) and the adoption of theoretical estimation schemes for case 2 (since it depends on the atom energy only) reduce the numerical errors.

Electronic configurations and spin multiplicities for the ground state of atoms are referred to in a book by Karplus and Porter.[14] For transition metals, spin multiplicities for cations are estimated by considering that the outer s electrons are removed first and then the d electrons. For the electronic configurations of metal atoms and cations, the electron populations among the three p orbitals and the five d orbitals should be equal if the spherical symmetry is conserved. In the present work, no restriction is imposed. So the obtained electron density does not satisfy exactly the spherical symmetry, but their energies are adopted intact.

For Ag complexes with nonaqueous ligands, the ligand exchange reactions are written individually by the following chemical equations, in terms of the hydrated complex and the hydrated ligand molecules or ions.

$$Ag(OH_2)_6^+ + 2(NH_3 \cdot 2H_2O) \rightarrow Ag(NH_3)_2(OH_2)_4^+ + 6H_2O$$

$$Ag(OH_2)_6^+ + 2(CN^- \cdot 2H_2O) \rightarrow Ag(CN)_2(OH_2)_4^- + 6H_2O$$

$$Ag(OH_2)_6^+ + 2(S_2O_3^{2-} \cdot 2H_2O) \rightarrow Ag(S_2O_3)_2(OH_2)_4^{3-} + 6H_2O$$

The ligand exchange energy is evaluated by eq 5, where $n = 0$, 1, and 2 for $L = NH_3$, CN^-, and $S_2O_3^{2-}$, respectively. Equations 4a and 4b are modified to eqs 6a and 6b.

$$\epsilon_{li-ex} = \epsilon[AgL_2(OH_2)_4^{(1-2n)}] + \epsilon[6H_2O] - \epsilon[Ag(OH_2)_6^+] - 2\epsilon[L^{n-} \cdot 2H_2O] \quad (5)$$

$$\Delta\epsilon = \epsilon_{cohe}^{expt} + \epsilon_{ion} + \epsilon_{hydra} + \epsilon_{li-ex} = \epsilon_{cohe}^{expt} - \epsilon[M^0] + \epsilon[M(OH_2)_6^{n+}] - \epsilon[6H_2O] + \epsilon_{li-ex} \quad (6a)$$

$$\Delta\epsilon = \epsilon_{cohe}^{expt} + \epsilon_{ion}^{expt} + \epsilon[M(OH_2)_6^{n+}] - \epsilon[M^{n+}] - \epsilon[6H_2O] + \epsilon_{li-ex} \quad (6b)$$

The solvent effects are taken into consideration in an indirect manner, that is, by the self-consistent reaction field method at the level of the polarized continuum model (PCM).[1-3] All the species except for the isolated metal atom M^0 and the metal ion M^{n+} appearing in eqs 2a to 6b are evaluated in solution.

There are three levels of calculation. The lowest level is that optimization is carried out in gas-phase and the optimized geometry is used for the PCM calculation without further optimization. We refer to this level of calculation as method-Hv. "H" means enthalpy, which is equal to the SCF energy if the change of volume is ignored. "v" represents that the geometry is optimized in "vacuum".

In the second level of calculation, the geometry is optimized under the PCM, and the corresponding label is method-Hp. "p" represents PCM. In the highest level of calculation, the geometry optimization is the same as the second level, i.e., under the PCM, and furthermore the harmonic frequency is calculated under the PCM to consider the zero point energy and the vibrational contribution of entropy. Small correction from translation and rotation contribution is estimated by the classical approximation. With the PCM, the harmonic frequency is evaluated by the calculus of finite difference of the energy gradient since the analytical second energy derivative is not available. This level of calculation is labeled as method-G, where "G" means the Gibbs free energy. In method-G, the thermal correction is also considered for free atoms and cations. We have the gas-phase results too, but we will not show them since they are far from experimental results. In the present model, electrons released from atoms are assumed to go away from the system, and the charging-up effects of electrodes are not considered.

According to the text book of physical chemistry or electrochemistry, the SRP or the standard hydrogen electrode (SHE) potential E_{SHE} is related to the free energy change $\Delta\epsilon$ by eq 7, where $\Delta\epsilon$ is represented in "eV" unit, and ν is the number of electrons transferred to cation. The absolute potential value for hydrogen electrode (4.43 V) is taken from the paper by Reiss and Heller.[15]

$$E_{SHE} = \left(\frac{\Delta\epsilon}{\nu|e|} - 4.43 \right) \qquad (7)$$

All the calculation is carried out with Gaussian 03 program package.[16] The Becke three-parameter Lee−Yang−Parr hybrid functionals are employed.[17−20] Two types of basis sets are used, i.e., all-electron 6-311G(d,p) and the Los Alamos model core potential (MCP).[21,22] Both basis sets have their limits of application. The all-electron 6-311G(d,p) basis is not applicable to the second and third row transition elements, and we treated 16 ions, Li^+, K^+, Ca^{2+}, Na^+, Mg^{2+}, Al^{3+}, Ti^{2+}, Mn^{2+}, Zn^{2+}, Cr^{3+}, Fe^{2+}, Co^{2+}, Ni^{2+}, Fe^{3+}, Cu^{2+}, and Cu^+ with this basis set. On the other hand, the MCP basis is not applicable to Li^+, Na^+, Mg^{2+}, and Al^{3+} ions because of no valence electrons, and we applied the MCP basis to the following 17 ions, K^+, Ca^{2+}, Ti^{2+}, Mn^{2+}, Zn^{2+}, Cr^{3+}, Fe^{2+}, Co^{2+}, Ni^{2+}, Fe^{3+}, Cu^{2+}, Cu^+, Ag^+, Pd^{2+}, Pt^{2+}, Au^{3+}, and Au^+. Several ions are dealt with by the both basis sets and could be compared to each other.

Results and Discussion

1. Isolated Ligand Systems. The optimized structures of water cluster $6H_2O$, and three ligand−water clusters $2(NH_3 \bullet 2H_2O)$, $2(CN^- \bullet 2H_2O)$, and $S_2O_3^{2-} \bullet 2H_2O$ are shown in Figure 2. All four structures are optimized in gas-phase or under the PCM depending on the methods. Except for $2(S_2O_3^{2-} \bullet 2H_2O)$, the whole structures $6H_2O$, $2(NH_3 \bullet 2H_2O)$, and $2(CN^- \bullet 2H_2O)$ are optimized, and their energies are used. However, the whole structure $2(S_2O_3^{2-} \bullet 2H_2O)$ could not be optimized. It separates into the two subunits $S_2O_3^{2-} \bullet 2H_2O$ probably due to the strong electrostatic repulsion between them, even in the PCM calculation. Then the optimization is carried out with the single subunit, and the energy is doubled to estimate that for $2(S_2O_3^{2-} \bullet 2H_2O)$.

2. SRPs for 21 Metal Ions. For 21 metal ions examined, three configurations of aqueous complexes are optimized in gas-phase, and then the energies of configurations are recalculated under the PCM. The most stable configuration is selected, and its energy is used to evaluate the SRP with methods-Hv. For methods-Hp and -G, the structure is optimized again under the PCM. Table 1 shows the spin multiplicity for atom and cation, the experimental values of cohesive energy and ionization energy, the most stable configuration of aqueous complex, and the experimental SRP value. The spin multiplicity and stable configuration are common to all the calculations. We consulted three experimental SRP values referred to as refs 7a−c. References 7a and 7b are almost the same, but that from ref 7c deviates from the former two to some degree. So the value from ref 7b is adopted as the reference experimental SRP value and cited in Table 1.

Table 2 shows the results of all-electron calculation for the 16 metals. It contains the hydration energy, (calculated) ionization energy, and SRP values with their deviations from the experimental value (ΔSRP), for the three methods. For Mn^{2+}, Zn^{2+}, Cr^{3+}, Fe^{2+}, Co^{2+}, Ni^{2+}, Cu^{2+}, and Cu^+, the ionization energies are underestimated, and the experimental ionization energy is employed. For other ions, the calculated ionization energy is employed. The largest discrepancy is
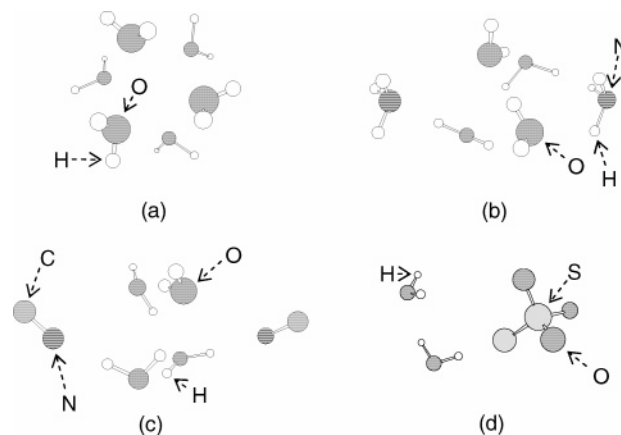
Figure 2. Optimized structures for water cluster and three ligand−water clusters with the lowest total energies: (a) $6H_2O$, (b) $2(NH_3 \bullet 2H_2O)$, (c) $2(CN^- \bullet 2H_2O)$, and (d) $S_2O_3^{2-} \bullet 2H_2O$.

Table 1. Name of Ion, Multiplicity of Atom and Ion, Experimental Cohesive Energy, Experimental Ionization Energy, Most Stable Configuration, and Experimental SRP Value

ion name	multiplicity[a]	cohesive energy[b]	ioniza. energy[c]	configuration[d]	exptl SRP value[e]
Li^+	2→1	1.63	5.392	4 + 2	−3.045
K^+	2→1	0.934	4.341	4 + 2	−2.925
Ca^{2+}	1→1	1.84	17.984	6 + 0	−2.84
Na^+	2→1	1.113	5.139	4 + 2	−2.714
Mg^{2+}	1→1	1.51	22.681	6 + 0	−2.356
Al^{3+}	2→1	3.39	53.261	6 + 0	−1.676
Ti^{2+}	3→3	4.85	20.40	6 + 0	−1.63
Mn^{2+}	6→6	2.92	23.075	6 + 0	−1.18
Zn^{2+}	1→1	1.35	27.358	6 + 0	−0.7626
Cr^{3+}	7→4	4.10	54.226	6 + 0	$(-0.740)^f$
Fe^{2+}	5→5	4.28	24.05	6 + 0	−0.440
Co^{2+}	4→4	4.39	24.96	6 + 0	−0.277
Ni^{2+}	3→3	4.44	25.803	6 + 0	−0.257
Fe^{3+}	5→6	4.28	54.701	6 + 0	$(-0.037)^g$
Cu^{2+}	2→2	3.49	28.018	6 + 0	0.340
Cu^+	2→1	3.49	7.726	2 + 4	0.520
Ag^+	2→1	2.95	7.576	2 + 4	0.7991
Pd^{2+}	1→1	3.89	27.77	4 + 2	0.915
Pt^{2+}	3→1	5.84	27.563	4 + 2	1.188
Au^{3+}	2→1	3.81		4 + 2	1.52
Au^+	2→1	3.81	9.225	2 + 4	1.83

[a] "M→N" means that the spin multiplicity for atom is M and that of cation is N. [b] Cohesive energy is taken from ref 9, and the unit is eV. [c] Experimental ionization energy taken from ref 7c, and the unit is eV. [d] Configuration symbols "6 + 0", "4 + 2", and "2 + 4" mean that number of H_2O molecules in the first coordination shell is 6, 4, and 2, respectively. [e] Unit is V. [f] Estimated from the two reaction, $Cr^{2+} + 2e^- = Cr$ and $Cr^{3+} + e^- = Cr^{2+}$. [g] Estimated from the two reaction, $Fe^{2+} + 2e^- = Fe$ and $Fe^{3+} + e^- = Fe^{2+}$.

found for Cu^+ throughout the three methods. The next ones are Al^{3+}, K^+, Li^+ and Co^{2+}, and their relative magnitude of deviation is changing depending on the methods. Raising the calculation level to method-Hp and method-G, the magnitude of discrepancy are almost the same. The standard deviation for the 16 metals is 0.20−0.22 V.

Table 3 shows the results of MCP calculation such as the hydration energy, ionization energy, and SRP with ΔSRP

Table 2. Name of Ion, Hydration Energy, Ionization Energy, SRP Values, and their Differences from Experimental Values Calculated with an All-Electron Basis Set[a]

ion	hydra. energy	ioniza. energy[b]	method-Hv		method-Hp		method-G	
			SRP	ΔSRP	SRP	ΔSRP	SRP	ΔSRP
Li^+	−6.12	5.62	−3.31	−0.26	−3.36	−0.31	−3.23	−0.19
K^+	−3.65	4.50	−2.65	0.27	−2.74	0.18	−2.67	0.25
Ca^{2+}	−16.88	18.24	−2.83	0.01	−2.88	−0.04	−3.00	−0.16
Na^+	−4.78	5.42	−2.68	0.04	−2.80	−0.08	−2.70	0.01
Mg^{2+}	−20.51	23.19	−2.34	0.02	−2.38	−0.03	−2.38	−0.03
Al^{3+}	−48.02	53.92	−1.33	0.34	−1.39	0.29	−1.29	0.39
Ti^{2+}	−19.41	20.50	−1.46	0.17	−1.52	0.11	−1.59	0.04
Mn^{2+}	−19.50	*23.06*	−1.18	−0.00	−1.23	−0.05	−1.28	−0.10
Zn^{2+}	−21.45	*27.13*	−0.80	−0.04	−0.84	−0.08	−0.81	−0.05
Cr^{3+}	−46.96	*53.96*	−0.64	0.10	−0.70	0.05	−0.64	0.10
Fe^{2+}	−20.51	*24.00*	−0.52	−0.08	−0.57	−0.13	−0.58	−0.14
Co^{2+}	−21.54	*24.87*	−0.52	−0.25	−0.58	−0.30	−0.54	−0.26
Ni^{2+}	−22.07	*25.66*	−0.34	−0.08	−0.39	−0.13	−0.32	−0.06
Fe^{3+}	−45.90	55.39	0.16	0.20	0.11	0.14	0.14	0.18
Cu^{2+}	−22.00	*26.36*	0.32	−0.02	0.28	−0.06	0.29	−0.05
Cu^+	−6.75	*7.18*	0.04	−0.48	−0.17	−0.69	−0.11	−0.63
StDev				0.20		0.22		0.22

[a] Units for hydration and ionization energies are in eV, and units for SRP and ΔSRP are in V. [b] For Mn^{2+}, Zn^{2+}, Cr^{3+}, Fe^{2+}, Co^{2+}, Ni^{2+}, Cu^{2+}, and Cu^+, calculated ionization energies (italicized) underestimate experimental ionization energy, and the SRP (and also ΔSRP) is evaluated using the experimental ionization energy.

Table 3. Name of Ion, Hydration Energy, Ionization Energy, SRP Values, and their Differences from Experimental Values Calculated with the MCP Basis Set[a]

ion	hydra. energy	ioniza. energy[b]	method-Hv		method-Hp		method-G	
			SRP	ΔSRP	SRP	ΔSRP	SRP	ΔSRP
K^+	−3.34	4.44	−2.39	0.53	−2.34	0.59	−2.29	0.63
Ca^{2+}	−16.36	18.21	−2.59	0.26	−2.55	0.32	−2.57	0.27
Ti^{2+}	−20.15	20.57	−1.80	−0.17	−1.78	−0.15	−1.78	−0.15
Mn^{2+}	−20.06	23.18	−1.41	−0.23	−1.38	−0.19	−1.42	−0.24
Zn^{2+}	−21.40	*26.38*	−0.78	-0.02	−0.74	0.02	−0.72	0.04
Cr^{3+}	−48.72	56.74	−0.39	0.35	−0.39	0.35	−0.28	0.46
Fe^{2+}	−21.13	*23.89*	−0.83	−0.39	−0.80	−0.36	−0.82	−0.38
Co^{2+}	−22.11	25.65	−0.47	−0.19	−0.43	−0.16	−0.43	−0.16
Ni^{2+}	−22.63	26.37	−0.34	−0.08	−0.30	−0.05	−0.32	−0.06
Fe^{3+}	−47.17	56.09	−0.03	0.01	−0.04	−0.00	0.04	0.07
Cu^{2+}	−22.46	28.60	0.39	0.05	0.42	0.08	0.39	0.05
Cu^+	−6.61	7.83	0.28	−0.24	0.35	−0.17	0.38	−0.14
Ag^+	−5.34	7.75	0.93	0.13	1.00	0.20	0.96	0.16
Pd^{2+}	−23.93	30.78	0.94	0.02	0.94	0.03	1.18	0.27
Pt^{2+}	−24.74	30.43	1.34	0.15	1.34	0.15	1.61	0.42
Au^{3+}	−50.30	66.03	2.09	0.57	1.93	0.41	1.96	0.44
Au^+	−6.86	9.42	1.94	0.11	1.99	0.16	1.99	0.16
StDev				0.23		0.23		0.27

[a] Units for hydration and ionization energies are in eV, and units for SRP and ΔSRP are in V. [b] For Zn^{2+} and Fe^{2+}, calculated ionization energies (italicized) underestimate experimental ionization energy, and the SRP (and also ΔSRP) is evaluated using the experimental ionization energy.

values evaluated by the three methods for the 17 metals. For Zn^{2+} and Fe^{2+}, the ionization energies are underestimated, and the experimental ionization energies are used. Throughout the three methods, the largest discrepancy is seen for
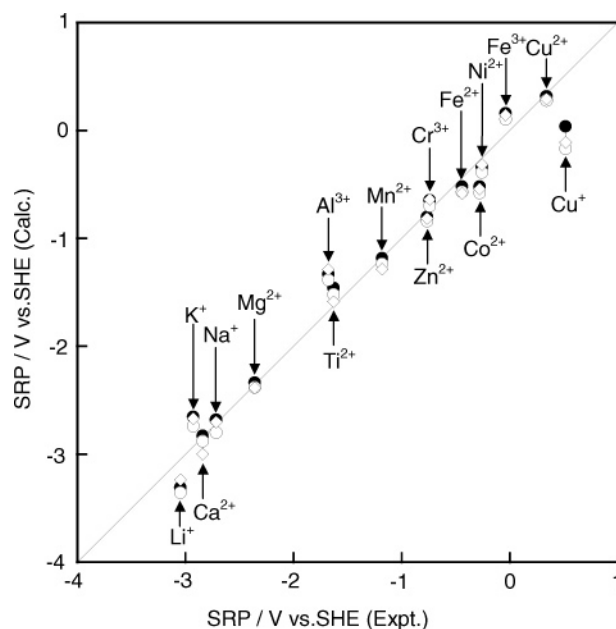
Figure 3. Correlation between three levels of calculated SRP and experimental SRP for 16 metal ions calculated with all-electron basis. Full circle, open circle, and open square represent values by methods-Hv, -Hp, and -G, respectively.
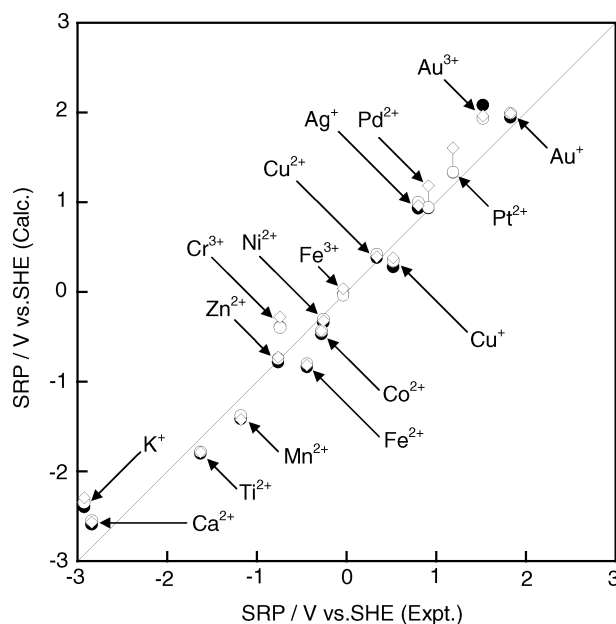
Figure 4. Correlation between three levels of calculated SRP and experimental SRP for 17 metal ions calculated with MCP basis. Full circle, open circle, and open square represent values by methods-Hv, -Hp, and -G, respectively.

Au^{3+}, K^+, and next Fe^{2+} and Cr^{3+}. In method-G, the agreement becomes worse even for Pt^{2+}. Thus the standard deviations are 0.23, 0.23, and 0.27 V for methods-Hv, -Hp, and -G, respectively.

Figures 3 and 4 show correlation relation between the calculated SRPs and the experimental SRP's. In the order of methods-Hv, -Hp, and -G, the computational cost increases, and the accuracy of calculated results is expected to be improved. Although the discrepancy is decreased for some ions, the overall consistency is not improved. Baik and

794 *J. Chem. Theory Comput., Vol. 3, No. 3, 2007*

Shimodaira et al.

Table 4. Energy Components To Evaluate SRP for Ag Complexes[a,b]

ligand	$2(L^{n-}\cdot 2H_2O)$	$AgL_2(OH_2)_4^{(1-2n)}$	ϵ_{li-ex}	SRP (calc)	SRP (expt)
NH_3; $n = 0$	−418.9058	−564.5968	−0.571	0.361	0.373
CN^-; $n = 1$	−491.6624	−637.3890	−1.538	−0.607	−0.310
$S_2O_3^{2-}$; $n = 2$	−797.7425	−943.4578	−1.157	−0.225	−0.017

[a] Units for $2(L^{n-}\cdot 2H_2O)$ and $AgL_2(OH_2)_4^{(1-2n)}$ are hartree (au), the unit for ϵ_{li-ex} is eV, and those for SRP(calc) and SRP(expt) are V. [b] Aqueous complex, $Ag(OH_2)_6^+$, and water cluster, $6H_2O$, are those used in the present work and common to three systems. Their energies are −604.3313 au and −458.6612 au, respectively. The sum of cohesive, ionization, and hydration energies for Ag, $\epsilon_{cohe}^{expt} + \epsilon_{ion} + \epsilon_{hydra}$, is taken from Table 3 and 5.36 eV.

Friesner also stated on this point.[9] In their words, there is another source of entropy such as reorientation of solvents, which is not taken into account by the vibrational analysis of solute. Unfortunately, cancellation of errors occurs, and the three methods afford the almost same results for the all-electron calculation, and methods-Hv and -Hp give better results than method-G for the MCP calculation.

3. SRPs for Three Ag Complexes. The ligand exchange reactions are dealt with at the level of method-Hv. The energies of aqueous complex and water cluster are same as those used in the previous section. The structures of three Ag complexes, $Ag(NH_3)_2(OH_2)_4^+$, $Ag(CN)_2(OH_2)_4^-$, and $Ag(S_2O_3)_2(OH_2)_4^{3-}$, where nonaqueous ligands occupy the trans position, are optimized in gas-phase, and then the energies are re-evaluated with the PCM. Several configurations for the ligand−water complexes are examined with the PCM, and the most stable configuration with the lowest energy is adopted as the reference, which is shown in Figure 2(b)−(d).

Table 4 shows the energies for ligand−water complex and Ag complex. Using these energies and the energies of aqueous complex and water cluster, the ligand exchange energy, ϵ_{li-ex}, is evaluated. Adding ϵ_{li-ex} to the sum of cohesive, ionization, and hydration energies, $\epsilon_{cohe}^{expt} + \epsilon_{ion} + \epsilon_{hydra}$, taken from Tables 1 and 3, the SRP is obtained after converting the energy to the electrochemical potential according to eq 7. For $[Ag(CN)_2(OH_2)_4]^-$ and $[Ag(S_2O_3)_2(OH_2)_4]^{3-}$, the discrepancy is smaller than 0.3 V, and an excellent agreement is obtained for $[Ag(NH_3)_2(OH_2)_4]^+$.

Conclusion

In this work, for the first time we presented the theoretical estimation of SRP concerning the process from bulk metal to metal ion and metal complex. The 21 metal ions and three Ag complexes were examined. Throughout the three levels of calculations, Cu^+ and Al^{3+} ions and K^+ and Au^{3+} ions indicated the worst agreement with the experimental data for the all-electron and MCP basis sets, respectively. The ill-tempered nature of Cu^+ was much improved for the MCP calculation. These ill-tempered ions increased the standard deviation and lowered the whole quality of calculations, although the agreement was given within 0.2 V, i.e., 4.6 kcal/mol for 11 and 10 ions with the all-electron and MCP basis

sets, respectively, in method-Hv. Except for method-G with the MCP basis set, the standard deviations were in the range of 0.20−0.23, and these are fairly good values. Although there is room to be improved, such as accurate evaluation of ionization energy and entropy contribution, it is a kind of surprise that we have reproduced the SRP by the DFT calculation based on a very simple idea, i.e., the Born−Harber cycle. In future works, detailed parts of the PCM parameter such as volume size should be optimized as well as a more careful selection of the exchange correlation functionals.

References

(1) (a) Miertus, S; Scrocco, E; Tomasi, J. *Chem. Phys.* **1981**, *55*, 117. (b) Miertus, S.; Tomasi, J. *Chem. Phys.* **1982**, *65*, 239.

(2) Friedrichs, M.; Zhou, R.; Edinger, S. R.; Friesner, R. A. *J. Phys. Chem. B* **1999**, *103*, 3057.

(3) Cossi, M.; Scalmani, G.; Rega, N.; Barone, V. *J. Chem. Phys.* **2002**, *117*, 43.

(4) Edinger, S. R.; Cortis, C.; Shenkin, P. S.; Friesner, R. A. *J. Phys. Chem. B* **1997**, *101*, 1190.

(5) Kubicki, J. D. *J. Phys. Chem. A* **2001**, *105*, 8756.

(6) Liptak, M. D.; Gross, K. C.; Seybold, P. G.; Feldgus, S.; Shields, G. C. *J. Am. Chem. Soc.* **2002**, *124*, 6421.

(7) Han, W.-G.; Liu, T.; Lovell, T.; Noodleman, L. *Inorg. Chem.* **2006**, *45*, 8533.

(8) Abreu, A. H. D.; Guimarães, L.; Duarte, H. A. *J. Phys. Chem. A* **2006**, *110*, 7713.

(9) Baik, M-H.; Friesner, R. A. *J. Phys. Chem. A* **2002**, *106*, 7407.

(10) Undsemaa, M.; Tamm, T. *J. Phys. Chem. A* **2003**, *107*, 9997.

(11) (a) Bard, A. J.; Faulkner L. R. In *Electrochemical Methods, Fundamentals and Applications,* 2nd ed.; John Wiley & Sons: U.S.A., 2001; pp 808−810. (b) In *Kagaku-binran; Kiso-hen, II,* Eds.; Chemical Society of Japan: Maruzen, Japan, 1984; pp 466−468. (c) In *CRC Handbook of Chemistry and Physics,* 66th ed.; Weast, R. C., Eds.; CRC Press: U.S.A., 1986; pp D-151−158.

(12) Kobayashi, H.; Miura, T.; Shimodaira, Y.; Kudo, A. *Chem. Lett.* **2004**, *33,* 1176.

(13) Kittel, C., In *Introduction to Solid State Physic*, 8th ed.; John Wiley & Sons: U.S.A., 2005; p 50.

(14) Karplus, M; Porter, R. N. In *Atoms and Molecules*; W. A. Benjamin: U.S.A., 1970; pp 202−207.

(15) Reiss, H.; Heller, A. *J. Phys. Chem.* **1985**, *89,* 4207.

(16) Frisch, M. J.; Trucks, G. W.; Schlegel, H. B.; Scuseria, G. E.; Robb, M. A.; Cheeseman, J. R.; Montgomery, J. A., Jr.; Vreven, T.; Kudin, K. N.; Burant, J. C.; Millam, J. M.; Iyengar, S. S.; Tomasi, J.; Barone, V.; Mennucci, B.; Cossi, M.; Scalmani, G.; Rega, N.; Petersson, G. A.; Nakatsuji, H.;

DFT Method Estimation of Standard Redox Potential

J. Chem. Theory Comput., Vol. 3, No. 3, 2007 **795**

Hada, M.; Ehara, M.; Toyota, K.; Fukuda, R.; Hasegawa, J.; Ishida, M.; Nakajima, T.; Honda, Y.; Kitao, O.; Nakai, H.; Klene, M.; Li, X.; Knox, J. E.; Hratchian, H. P.; Cross, J. B.; Adamo, C.; Jaramillo, J.; Gomperts, R.; Stratmann, R. E.; Yazyev, O.; Austin, A. J.; Cammi, R.; Pomelli, C.; Ochterski, J. W.; Ayala, P. Y.; Morokuma, K.; Voth, G. A.; Salvador, P.; Dannenberg, J. J.; Zakrzewski, V. G.; Dapprich, S.; Daniels, A. D.; Strain, M. C.; Farkas, O.; Malick, D. K.; Rabuck, A. D.; Raghavachari, K.; Foresman, J. B.; Ortiz, J. V.; Cui, Q.; Baboul, A. G.; Clifford, S.; Cioslowski, J.; Stefanov, B. B.; Liu, G.; Liashenko, A.; Piskorz, P.; Komaromi, I.; Martin, R. L.; Fox, D. J.; Keith, T.; Al-Laham, M. A.; Peng, C. Y.; Nanayakkara, A.; Challacombe, M.; Gill, P. M. W.; Johnson, B.; Chen, W.; Wong, M. W.; Gonzalez, C.; Pople, J. A. *Gaussian 03*, *Revision B.03*; Gaussian, Inc.: Pittsburgh, PA, 2003.

(17) Becke, A. D. *Phys. Rev. A* **1988**, *38,* 3098.

(18) Lee, C.; Yang, W.; Parr, R. G. *Phys. Rev. B* **1988**, *37,* 785.

(19) Becke, A. D. *J. Chem. Phys.* **1993**, *98,* 1372.

(20) Gill, P. M. W.; Johnson, B. G.; Pople, J. A. *Int. J. Quantum Chem. Symp.* **1992**, *26,* 319.

(21) Hay, P. J.; Wadt, W. R. *J. Chem. Phys.* **1985**, *82,* 270; **1985**, *82,* 299.

(22) Dunning, T. H. J.; Hay, P. J. In *Modern Theoretical Chemistry;* Schaefer, H. F., III, Ed.; Plenum Press: New York, 1976; pp 1−35.